Biochemical and Biophysical Research Communications 431 (2013) 176–180

Contents lists available at SciVerse ScienceDirect

Biochemical and Biophysical Research Communications

journal homepage: www.elsevier.com/locate/ybbrc

His267 is involved in carbamylation and catalysis of RuBisCO-like protein from *Bacillus subtilis*

Toshihiro Nakano [a,1], Yohtaro Saito [a], Akiho Yokota [a], Hiroki Ashida [a,b,*]

[a] Graduate School of Biological Sciences, Nara Institute of Science and Technology (NAIST), Ikoma, Nara 630-0192, Japan
[b] Precursory Research for Embryonic Science and Technology (PRESTO), Japan Science and Technology Agency (JST), 4-1-8 Honcho Kawaguchi, Saitama 332-0012, Japan

ARTICLE INFO

Article history:
Received 12 December 2012
Available online 9 January 2013

Keywords:
RuBisCO-like protein
RuBisCO
Bacillus subtilis
2,3-Diketo-5-methylthiopentyl-1-phosphate enolase
Carbamylation

ABSTRACT

Ribulose-1,5-bisphosphate carboxylase/oxygenase (RuBisCO) and RuBisCO-like protein (RLP) from *Bacillus subtilis* catalyze mechanistically similar enolase reactions. Both enzymes require carbamylation of the ε-amino group of the active site lysine during activation to generate the binding site of the essential Mg^{2+} ion. His267 forms a possible hydrogen bond with the carbamate of the active site Lys176 in *B. subtilis* RLP. This active site histidine is completely conserved in RLPs and RuBisCO. H267Q, H267N and H267A mutant enzymes required higher CO_2 concentrations for maximal activity than wild-type enzyme, suggesting that the histidine is involved in high affinity for activator CO_2 in *Bacillus* RLP. These mutations showed weak effects on the catalysis of RLP, whereas this residue is reportedly essential for catalysis in RuBisCO but is not involved in the carbamylation. The different functions of the active site histidine in RLP and RuBisCO are discussed.

1. Introduction

Ribulose-1,5-bisphosphate carboxylase/oxygenase (RuBisCO) plays a central role in carbon assimilation by fixing gaseous CO_2 into ribulose-1,5-bisphosphate (RuBP) in the Calvin cycle [1,2]. The carboxylation reaction entails the initial enolization of RuBP to give a *cis*-endiol intermediate and subsequent CO_2 addition, hydration, C2-C3 bond cleavage and stereospecific protonation, resulting in two molecules of 3-phosphoglycerate (Fig. S1A) [1,3]. RuBisCO is divided into three forms based on the amino acid sequence of the large subunit; form I from higher plants, algae, cyanobacteria and photosynthetic bacteria, form II from photosynthetic bacteria, and the archaeal form III [4]. All forms of RuBisCO require an activation process to be catalytically competent. Structural information and chemical modification of the active-site residues have revealed that RuBisCO activation occurs by reversible covalent binding of an activator CO_2 molecule to the ε-amino group of Lys201 (all sequence numbering of RuBisCO is based on the amino acid sequence of spinach RuBisCO unless otherwise stated) to form a carbamate (producing the unstable EC form) [1,2,5]. Subsequently, the carbamylated Lys201, together with Asp203 and Glu204, coordinates a catalytically essential Mg^{2+} ion to produce the active ECM form (Fig. 1A) [1,2,6]. The carbamylated Lys201 also acts as the general base to abstract the C3-proton of RuBP in the initial enolization [1–3]. Therefore, the carbamylation of the lysyl residue is the transition point from the inactive form to the active form of RuBisCO.

RuBisCO-like proteins (RLPs) are members of the RuBisCO superfamily that share a common ancestral protein, based on structural similarity and ~25% sequence homology in both proteins [4,6,7]. RLPs catalyze neither carboxylation nor oxygenation of RuBP, but conserve 9–18 of the 19 catalytic residues of RuBisCO, including the active site lysine for carbamylation [4,7]. In our previous study, the catalytic function of RLP was first revealed in *Bacillus subtilis*; it catalyzes the enolization of 2,3-diketo-5-methylthiopentyl-1-phosphate (DK-MTP-1-P) in the methionine salvage pathway, a reaction similar to RuBP enolization by RuBisCO (Fig. S1B) [7–11]. The enolization of DK-MTP-1-P is also catalyzed by RLPs from *Microcystis aeruginosa* and *Geobacillus kaustophilus* [11–13]. Recently, it was revealed that RLP of *Rhodospirillum rubrum* catalyzes similar but different reaction, isomerization of 5-methylthioribulose-1-phosphate (MTRu-1-P) in the proposed 5-methylthioadenosine-isoprenoid metabolism [14]. Like RuBisCO, *Bacillus subtilis* RLP (BsRLP) structurally conserves $Lys176^{Bs}$, $Asp178^{Bs}$ and $Glu179^{Bs}$ (the superscript Bs indicates residue

Abbreviations: CABP, 2-carboxy-D-arabinitol-1,5-bisphosphate; DK-H-1-P, 2,3-diketohexane-1-phosphate; DK-MTP-1-P, 2,3-diketo-5-methylthiopentyl-1-phosphate; RuBP, ribulose-1,5-bisphosphate; RuBisCO, Ribulose-1,5-bisphosphate carboxylase/oxygenase; RLP, RuBisCO-like protein.

* Corresponding author. Address: Graduate School of Biological Sciences, Nara Institute of Science and Technology (NAIST), 8916-5 Takayama-cho, Ikoma, Nara 630-0192, Japan. Fax: +81 743 72 5569.
E-mail address: ashida@bs.naist.jp (H. Ashida).
[1] Present address: Pharmaceuticals Research Center, Asahi Kasei Pharma Corp., Izunokuni, Shizuoka 410–2321, Japan.

0006-291X/$ - see front matter © 2013 Elsevier Inc. All rights reserved.
http://dx.doi.org/10.1016/j.bbrc.2012.12.142

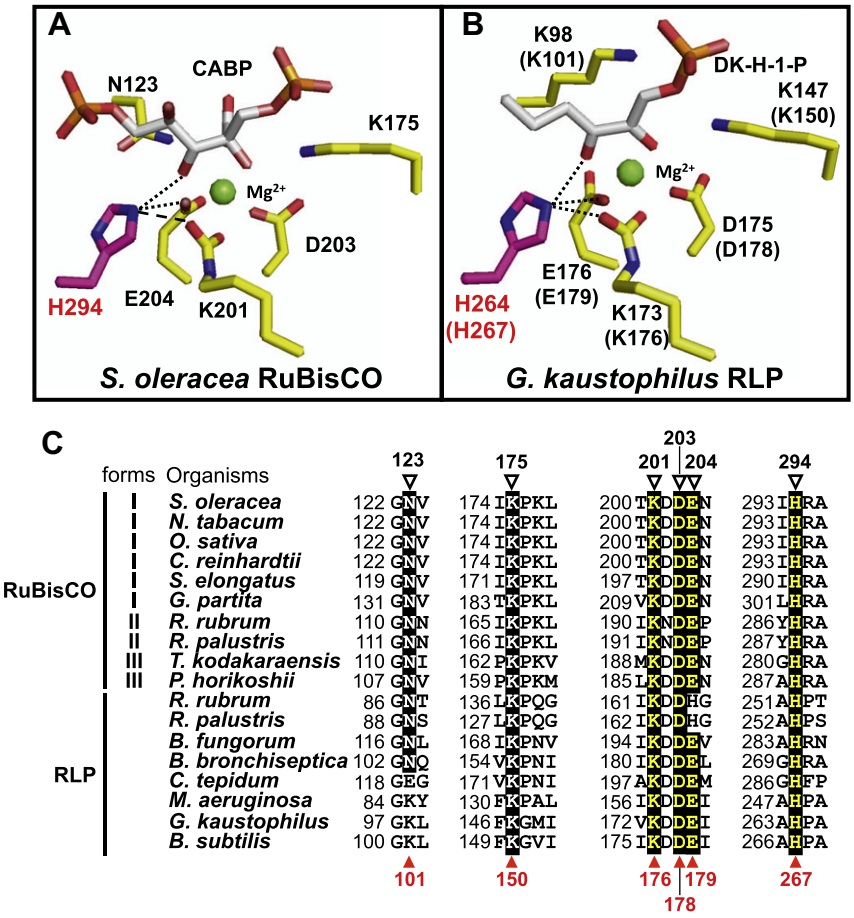

Fig. 1. Active sites of RuBisCO and RLP. (A) ECM form complexed with transition-state analog 2-carboxy-D-arabinitol-1,5-bisphosphate (CABP; Fig. S1C) of *Spinacia oleracea* RuBisCO (PDB: 8RUC) and (B) the ECM form complexed with substrate analog 2,3-diketohexane-1-phosphate (DK-H-1-P; Fig. S1C) of *Geobacillus kaustophilus* RLP (PDB: 2OEM). Hydrogen-bonding interactions of the active site histidine are shown as dotted (<3.3 Å) and dashed (3.56 Å) lines. Green spheres indicate Mg^{2+} ions. Number in parentheses represents amino acid residue in *B. subtilis* RLP. (C) Partial amino acid sequence alignment around active site residues of RLPs and RuBisCOs. Conserved catalytic residues essential for the RuBisCO carboxylation are highlighted in black. Lys201, Asp203, Glu204, and His294 are colored yellow. RLP and RuBisCO amino acid sequences were obtained from the following organisms: *S. oleracea* (NP_054944), *Nicotiana tabacum* (NP_054507), *Oryza sativa* Japonica Group (NP_039391), *Chlamydomonas reinhardtii* (NP_958405), *Synechococcus elongatus* PCC6301 (YP_170840), *Galdieria partita* (BAA75796), *Rhodospirillum rubrum* ATCC11170 (form II, YP_427487; RLP, YP_427085), *Rhodopseudomonas palustris* CGA009 (form II, NP_949975; RLP, NP_947514). *Thermococcus kodakaraensis* KOD1 (YP_184703), *Pyrococcus horikoshii* OT3 (NP_142861), *Burkholderia fungorum* (D9N172_9BURK), *Bordetella bronchiseptica* RB50 (NP_887583), *Chlorobium tepidum* TLS (NP_662651), *Microcystis aeruginosa* PCC7806 (CAJ43366), *G. kaustophilus* HTA426 (YP_146806), *B. subtilis* str. 168 (NP_389242). Sequences are numbered above the alignment according to the *S. oleracea* RuBisCO sequence. The sequence numbers shown in red at the bottom are according to the *B. subtilis* RLP sequence. Numbers to the left of sequences indicate the actual number in each protein. (For interpretation of the references to color in this figure legend, the reader is referred to the web version of this article.)

number in BsRLP; equivalent to Lys201, Asp203, and Glu204 in RuBisCO; Fig. 1C), which are superimposable on residues at the active site of RuBisCO [11,15]. Further mutational and enzymatic analyses of BsRLP showed that these residues and Mg^{2+} ions are essential for catalysis [11]. In the structure of *G. kaustophilus* RLP (GkRLP; PDB: 2OEM and 2OEK) crystallized with bicarbonate, the ε-amino group of $Lys173^{Gk}$ (the superscript Gk indicates residue number in GkRLP; equivalent to Lys201 in RuBisCO) is carbamylated and coordinates the Mg^{2+} together with $Asp175^{Gk}$ and $Glu176^{Gk}$ (equivalent to Asp203 and Glu204 in RuBisCO; Fig. 1C) in a similar manner to RuBisCO (Fig. 1B) [13]. These facts suggest that RLPs and RuBisCO utilize a structurally similar active site for enolization [7–9].

One of the active site residues, His294, is placed in the vicinity of the carbamate oxygen of Lys201 (Fig. 1) and forms hydrogen-bonding interactions with the C3-hydroxyl group of RuBP and the side chains of the metal-coordinating residues, carbamylated Lys201 and Glu204 in RuBisCO. In RuBisCO, it has been proposed that His294 plays multiple catalytic roles in the overall carboxylase reaction – enolization, carboxylation, hydration, and C2–C3 bond cleavage – but is not involved in the carbamylation [16]. Interestingly, this histidine is evolutionarily completely conserved in the RuBisCO superfamily (Fig. 1C), although RLPs as DK-MTP-1-P enolases catalyze only enolization (Fig. S1). The conservation of the histidine invites consideration of the evolutionary and functional relationships in the RuBisCO superfamily, but the function of this residue is unknown in RLPs. Here, we report the function of $His267^{Bs}$ (equivalent to His294 in RuBisCO; Fig. 1) in BsRLP as revealed by mutational analysis.

2. Materials and methods

2.1. Site-directed mutagenesis

Insertion of the *mtnW* gene encoding BsRLP into the pET15b vector (Novagen, Madison, WI) to give pET15b-mtnW was described previously [9]. Site-directed mutagenesis at His267 to produce H267Q, H267N, and H267A mutants of BsRLP using pET15b-mtnW as a template was performed by whole-plasmid

PCR with KOD DNA Polymerase plus (Toyobo, Osaka, Japan). The thermo-cycling program was as follows: 30 cycles of denaturation at 94 °C for 30 s, annealing at 55 °C for 30 s and elongation at 68 °C for 7 min. The mutagenic primer sets used for PCR were as follows: H267Q-forward, GATTATGGCGCAACCAGCAGTGAG; H267N-forward, GATTATGGCGAATCCAGCAGTGAG; H267A-forward, GATTATGGCGGCTCCAGCAGTGAG; H267- common reverse, GGAAC TGGGATTTCAGGATCTTCTGC. PCR products were phosphorylated at the 5′ end with T4 polynucleotide kinase (Takara Bio, Ohtsu, Japan), ligated with Ligation High (Toyobo), and transformed into *Escherichia coli* DH5α (Novagen). Successful mutagenesis was confirmed by sequencing with a 3100 Genetic Analyzer (Applied Biosystems, Tokyo, Japan).

2.2. Expression, purification and PAGE analyses of wild-type and mutant enzymes

E. coli BL21 (DE3; Novagen) transformed with the expression vector was grown at 25 °C for 12 h in 100 mL of LB medium containing 50 μg mL^{-1} ampicillin and 1 mM isopropyl β-D-thiogalactopyranoside. Wild-type and His267 mutants enzymes were purified from crude extract as described previously [10,11]. Sodium dodecyl sulfate (SDS) and native polyacrylamide gel electrophoresis (PAGE) was carried out (Fig. S2A, B) as described previously [10].

2.3. Enzyme assays

The DK-MTP-1-P enolase activity of wild-type and mutant BsRLP enzymes was measured as described previously [11]. Before activity assay, 70 μg of enzyme was activated in 100 μL of 50 mM Tris–HCl (pH 8.2), 25 mM $NaHCO_3$ and 20 mM $MgCl_2$ for 20 min at 25 °C, and an aliquot was used for assay. The enolase reaction was initiated by adding 1.6 μg of MTRu-1-P dehydratase to a reaction mixture containing 50 mM Tris–HCl (pH 8.2), 25 mM $NaHCO_3$, 20 mM Mg^{2+} and various concentrations of MTRu-1-P. The final reaction volume was 100 μL and the reaction temperature was 35 °C. The amount of the product, 2-hydroxy-3-keto-5-methylthiopentenyl-1-phosphate, was monitored spectrophotometrically at 280 nm with a UV–visible spectrophotometer (Hewlett Packard, Palo Alto, CA). The substrate and coupling enzyme were prepared as described previously [9,11].

The effect of CO_2 and $MgCl_2$ concentrations on the enolase activities of wild-type and mutant enzymes was examined under standard (20 mM Mg^{2+}, 25 mM $NaHCO_3$), low Mg^{2+} (1 mM Mg^{2+}, 25 mM $NaHCO_3$), low CO_2 (20 mM Mg^{2+}, no $NaHCO_3$ added), or low Mg^{2+} and CO_2 (1 mM Mg^{2+}, no $NaHCO_3$ added) conditions. To evaluate enolase activity, 70 μg of RLP in 100 μL of 50 mM Tris–HCl (pH 8.2) was pre-incubated for 20 min at 25 °C for each of the conditions. Aliquots of incubated enzyme were used to measure the enolase activity under the same conditions as the pre-incubation. Activities were normalized against the level of activity measured after pre-incubation under standard conditions for each enzyme.

Under these reaction conditions, the overall coupling reaction was limited by the amount of RLP.

3. Results and discussion

3.1. Interactions of the active site histidine in RLP

In the ECM form (PDB: 2OEK) and the ECM form complexed with substrate analog 2,3-diketohexane-1-phosphate (DK-H-1-P; Fig. S1C) of GkRLP (ECM-suba; PDB: 2OEM), $His264^{Gk}$ approximates the active site with the Mg^{2+} ion coordinated by carbamylated $Lys173^{Gk}$, $Asp175^{Gk}$, and $Glu176^{Gk}$ (Fig. 1B and Table S1). The NE2 imidazol nitrogen of $His264^{Gk}$ forms hydrogen bonds with the carbamate oxygen of $Lys173^{Gk}$ (2.84 Å in ECM and 3.14 Å in ECM-suba forms) and the carboxyl oxygen of $Glu176^{Gk}$ (3.18 Å in ECM and 2.96 Å in ECM-suba forms) [13]. $His264^{Gk}$ also forms a hydrogen bond with the C3-carbonyl oxygen of DK-H-1-P (2.77 Å in ECM-suba form). These facts suggested that the histidine is involved in carbamylation and catalysis in RLP.

3.2. Expression and purification of wild-type and His267 mutant enzymes of BsRLP

To analyze the catalytic role of this histidine in BsRLP, we replaced the histidine at position 267 with glutamine or asparagine to retain the hydrogen bonding potential, or alanine to disrupt the hydrogen-bonding interaction. Wild-type and mutant enzymes were expressed in *E. coli*. The identical mobilities of wild-type and mutant enzymes on an SDS–PAGE gel suggested that these proteins had not undergone proteolysis (Fig. S2A). Purified mutant enzymes showed similar mobilities to wild-type enzyme during non-denaturing electrophoresis, suggesting that all mutants formed stable catalytic dimers (Fig. S2B). These mutations might have affected the formation of an active conformation but the H267Q mutant had only slightly lower mobilities than wild-type protein, probably because of small structural change caused by alteration of the side chain at position 267.

3.3. His267 is involved in carbamylation of Lys176 in BsRLP

To analyze the functional interaction between $His267^{Bs}$ and the carbamate oxygen, we first examined the CO_2 and Mg^{2+} concentration requirements for activity in the wild-type and His267 mutant enzymes (Fig. 2). The activities of the wild-type and mutant enzymes were normalized to 100% after pre-incubation in 25 mM $NaHCO_3$ and 20 mM $MgCl_2$ (standard conditions). $MgCl_2$ and $NaHCO_3$ concentrations had no significant effect on wild-type activity. In contrast, $His267^{Bs}$ mutant enzymes required high CO_2 and Mg^{2+} concentrations, and showed only 10% activity under low Mg^{2+} and CO_2 conditions (1 mM $MgCl_2$, no $NaHCO_3$ added). In particular, low CO_2 conditions (20 mM $MgCl_2$, no $NaHCO_3$ added) caused severe reduction of mutant activities to 20% of the fully-activated enzymes. The mutant enzymes also exhibited 57–89% activity under low Mg^{2+} conditions (1 mM Mg^{2+} and 25 mM $NaHCO_3$). $MgCl_2$ and $NaHCO_3$ were inhibitory above the concentrations of the standard conditions in the mutant enzymes (data not shown) and therefore the Mg^{2+} and CO_2 concentrations of the

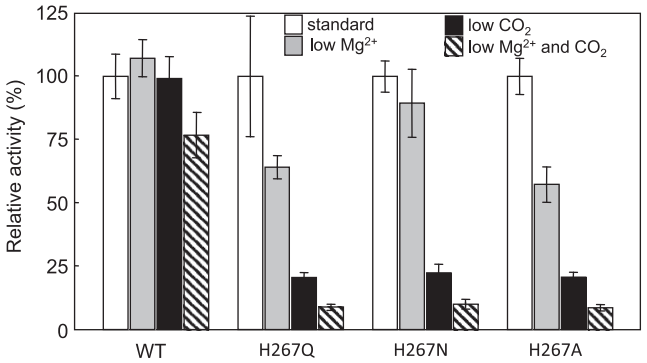

Fig. 2. Effects of CO_2 and Mg^{2+} concentrations on the enolase activity of wild-type (WT) and His267 mutants. The activities were measured at 35 °C after preincubation at 25 °C for 20 min under standard (20 mM $MgCl_2$ and 25 mM $NaHCO_3$), low CO_2 (20 mM $MgCl_2$, no $NaHCO_3$ added), low Mg^{2+} (1 mM $MgCl_2$ and 25 mM $NaHCO_3$) or low CO_2 and Mg^{2+} (1 mM $MgCl_2$, no $NaHCO_3$ added) conditions. Data are the means ± SD of three independent experiments.

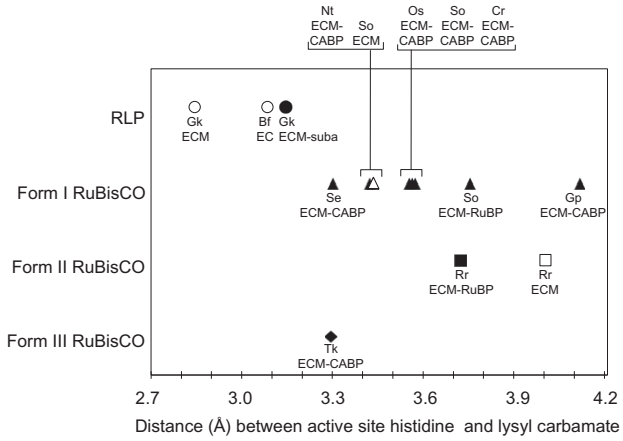

Fig. 3. Natural variations in the distance between the NE2 imidazol nitrogen of the active site histidine and the oxygen of the lysyl carbamate in X-ray crystallographic structures of RLPs and RuBisCOs. See Table S1 for a listing of the data, structural information and their sources. The distances were measured in 3D structures from: Gk, *G. kaustophilus* (RLP); Bf, *B. fungorum* (RLP); So, *S. oleracea* (form I RuBisCO); Nt, *N. tabacum* (form I); Os, *O. sativa* (form I); Cr, *C. reinharditii* (form I); Se, *S. elongatus* (form I); Gp, *G. partita* (form I); Rr, *R. rubrum* (form II); Tk, *T. kodakaraensis* (form III). Open circles (○), ECM and EC forms of RLPs; filled circle (●), ECM-suba form of RLP; open triangle (△), ECM form of form I RuBisCO; filled triangles (▲), ECM-RuBP and -CABP forms of form I RuBisCOs; open square (□), ECM form of form II RuBisCO; filled square (■), ECM-RuBP form of form II RuBisCO; filled diamond (♦), ECM-CABP form of form III RuBisCO.

standard conditions were enough for maximum activities in the mutant enzymes, as well as the wild-type enzyme. Thus, $His267^{Bs}$ mutants required higher Mg^{2+} and CO_2 concentrations for maximum activity than the wild-type. These results suggested that BsRLP requires activation through the carbamylation of $Lys176^{Bs}$ (equivalent to Lys201 in RuBisCO) for catalytic activity. Furthermore, large decreases in the enolase activity of the mutants under low CO_2 conditions indicated that $His267^{Bs}$ is involved in the affinity for activator CO_2 and/or stabilization of the carbamate through hydrogen-bonding interaction with the carbamate oxygen of $Lys176^{Bs}$. The H267N mutant showed a higher activity than the other two mutant enzymes under low Mg^{2+} conditions, but did not show any significant difference under low CO_2 and Mg^{2+} and low CO_2 conditions. This result indicated that the amide nitrogen of asparagine partially fulfilled a hydrogen-bonding role and was spatially equivalent to the imidazole nitrogen of histidine. The carbamate oxygens contact with not only $His264^{Gk}$ (2.84 Å in ECM and 3.14 Å in ECM-suba forms) but also $Ile145^{Gk}$ (equivalent to Ile148 in BsRLP; 3.50 Å in ECM and 3.36 Å in ECM-suba forms), $Asp175^{Gk}$ (equivalent to Asp178 in BsRLP; 2.78 Å in ECM and 3.03 Å in ECM-suba forms), $Glu176^{Gk}$ (equivalent to Glu179 in BsRLP; 2.77 Å in ECM and 2.81 Å in ECM-suba forms) and $Leu298^{Gk}$ (equivalent to Leu301 in BsRLP; 3.85 Å in ECM and 4.43 Å in ECM-suba forms) in GkRLP, suggesting that these residues also contribute to stabilize carbamylation in the active site lysine. Considering our results of mutant analysis, $His267^{Bs}$ largely contributes to stabilize the carbamate together with $Ile148^{Bs}$, $Asp178^{Bs}$, $Glu179^{Bs}$ and $Leu301^{Bs}$ in BsRLP.

Recently, the structure of *Burkholderia fungorum* RLP of unknown function was reported (PDB: 3NWR). In this enzyme, Lys195 (equivalent to Lys201 in RuBisCO) was carbamylated without Mg^{2+} coordination, resulting in the EC form. The distance between His284 (equivalent to His294 in RuBisCO) and the carbamate oxygen was 3.08 Å, indicating that His284 perhaps facilitates and stabilizes carbamate in the absence of Mg^{2+} (Table S1 and Fig. 3). This observation supports the hypothesis we propose in this report. Carbamylated lysine is found not only in RLP and RuBisCO but also in urease and phosphoesterase [3]. In the latter enzyme, the active-site histidine interacts with the carbamate oxygen to form a hydrogen bond [17,18]. Thus, a stabilizing mechanism for carbamate by the interaction of histidine seems to be utilized in various enzymes.

On the other hand, the distances between His294 and the carbamate in RuBisCOs are much longer (3.43 and 4.00 Å in the ECM forms of spinach and *R. rubrum* RuBisCO, respectively) than those of RLPs (Table S1 and Fig. 3) [19,20]. The distances in RuBisCO ECM forms complexed with RuBP (ECM-RuBP) and transition-state analog 2-carboxy-D-arabinitol-1,5-bisphosphate (CABP; Fig. S1C; ECM-CABP) are also longer than in the ECM-suba form of GkRLP. These facts suggest that interactions between the histidine and carbamate in RuBisCO are weaker than those in any forms of RLP. Interestingly, wild-type BsRLP under CO_2-free conditions with low CO_2 contamination (1.8 μM) still retained 77% activity of the enzyme under a high CO_2 concentration (80 μM, by addition of 10 mM $NaHCO_3$) [11]. Contrary to the high activation level of BsRLP under low CO_2 concentrations, form I spinach RuBisCO showed only 18% of total active sites were carbamylated at low (2 μM) CO_2 concentration in the presence of 20 mM Mg^{2+} [21]. Our results, together with these facts, suggested that the interaction between the histidine and carbamate should enable full activation of RLP under low CO_2 concentrations. Conversely, the weak interaction in RuBisCO may cause a low activation level under low CO_2 conditions. In fact, equilibrium constants for CO_2 activation in spinach and soybean RuBisCOs are 309 and 91 μM, respectively [21,22]. In form II RuBisCO from *R. rubrum*, the equilibrium constant for activator CO_2 (607 μM) is 1.9–6.6-fold higher than in plant RuBisCOs [23]. The side chain of the histidine in the ECM form of *R. rubrum* RuBisCO is placed 4 Å from the carbamylated lysine (Fig. 3 and Table S1). Considering that the equilibrium constant for activator CO_2 in BsRLP should be much lower than in RuBisCOs, the distance between the imidazole nitrogen of the histidine and the carbamate oxygen may correlate with the affinity for activator CO_2. Consequently, the strength of interaction between the histidine and carbamate probably determines the carbamate stability in RLPs and RuBisCOs.

3.4. Effect of His267 mutations on catalysis of BsRLP

We next determined the kinetic parameters of the $His267^{Bs}$ mutant enzymes after pre-incubation under standard conditions for full activation (Table 1). The H267Q, H267N and H267A mutations decreased k_{cat} to 2.2%, 8.1% and 7.4%, respectively, of the wild-type enzyme. In addition, the substitutions of $His267^{Bs}$ partially fulfilled or disrupted the hydrogen bond with the C3-carbonyl oxygen of the substrate (Fig. 1B), causing H267Q, H267N and H267A to show 2.6-, 2.2- and 3.0-fold increases in K_m. Therefore, the hydrogen bonding of $His267^{Bs}$ is involved in the affinity for the substrate. The H267Q, H267N and H267A mutations resulted in decreases to 0.8%, 3.7% and 2.4%, respectively, of the wild-type enzyme for k_{cat}/K_m. These results suggested that $His267^{Bs}$ is involved in

Table 1
Kinetic properties of wild-type and His267 mutant enzymes of BsRLP at 35 °C and pH 8.2.

Enzyme	k_{cat} (s^{-1}) [a]	K_m (μM) [a]	k_{cat}/K_m($M^{-1}s^{-1}$) [b]
Wild-type	78 ± 7.4	16 ± 4	4.9×10^6
H267Q	1.7 ± 0.2	42 ± 8	4.0×10^4
H267N	6.3 ± 0.3	35 ± 6	1.8×10^5
H267A	5.8 ± 0.3	48 ± 6	1.2×10^5

[a] Values are the means ± SD of three independent assays.
[b] Calculated values.

catalysis and substrate binding. The large decrease in k_{cat}/K_m of H267Q suggested that substitution to glutamine disrupts the active site, as observed in the lower mobility of the H267Q mutant enzyme than the others in non-denaturing electrophoresis (Fig. S2B).

Mutational approaches have revealed that *R. rubrum* RuBisCO mutants of His287 (equivalent to His294 in spinach RuBisCO; Fig. 1C), H287Q and H287N, are severely impaired in overall carboxylase (<0.001% and ~0.05% of the wild-type enzyme, respectively) and enolase activity (~0.1% of wild-type enzyme) [16], showing that the histidine is essential for catalysis. Based on these results, structural information and computational investigation, it has been proposed that His294 of RuBisCO plays multiple roles in the overall carboxylase reaction, specifically in the enolization, carboxylation, hydration, and C2-C3 cleavage steps. In the RuBP enolization step of RuBisCO, His294 probably promotes basicity of the carbamate oxygen of Lys201 through their interaction, and indirectly facilitates the proton abstraction performed by carbamylated Lys201 [16,24]. After the enolization, His294 initiates CO_2 addition by abstracting the O3 proton of *cis*-endiol and subsequently reprotonates O3 to generate gem-diol in the hydration step. In the last step, His294 also triggers C2–C3 bond cleavage by abstracting the O3 proton of gem-diol. The general base for DK-MTP-1-P enolization is still unclear in BsRLP. However, considering that mutants of $His267^{Bs}$ were impaired in enolase activity, carbamylated $Lys176^{Bs}$ may be a general base in BsRLP in a manner similar to carbamylated Lys201 in the RuBP enolization by RuBisCO. However, $Lys98^{Gk}$, conserved among DK-MTP-1-P enolases including BsRLP, was proposed as a general base in GkRLP based on structural and mutational analyses [13]. The general base residue of BsRLP remains to be revealed in future work. On the other hand, mutations showed weaker effects on the catalysis of RLP than of RuBisCO, suggesting that the contribution of $His267^{Bs}$ to catalysis in fully activated BsRLP is small.

3.5. Conclusion

The active site histidine, $His267^{Bs}$, is involved in carbamylation and catalysis in *B. subtilis* RLP. Hitherto, a residue directly involved in the carbamylation of Lys201 has not been reported in RuBisCO. We identified $His267^{Bs}$ as the residue that promotes or stabilizes carbamylation by increasing affinity for activator CO_2 through hydrogen-bonding interactions in RLP. However, the contribution of His294 to carbamylation should be smaller in RuBisCO because of the longer distance between His294 and the carbamate than RLPs. In contrast to carbamylation, the contribution of His294 to catalysis is larger in RuBisCO. For RuBisCO to have acquired the ability to catalyze the carboxylase reaction during its molecular evolution, His294 might have had multiple roles, such that location of this residue to a position further from the carbamate oxygen. Such a molecular evolutionary event might have imposed a high CO_2 concentration requirement for activation on RuBisCO. The active site histidine may contribute to the diversity of catalytic reactions and activation kinetics in RuBisCOs and RLPs.

Acknowledgments

This work was supported by the Japanese Society for the Promotion of Science (grant nos. 21688024 and 18688021 for Scientific Research), by the Nissan Science Foundation, by the Global COE Program at NAIST and the JST, PRESTO.

Appendix A. Supplementary data

Supplementary data associated with this article can be found, in the online version, at http://dx.doi.org/10.1016/j.bbrc.2012.12.142.

References

[1] F.C. Hartman, M.R. Harpel, Structure, function, regulation, and assembly of D-ribulose-1,5-bisphosphate carboxylase/oxygenase, Annu. Rev. Biochem. 63 (1994) 197–234.
[2] H. Roy, T.J. Andrews, Rubisco: assembly and mechanism, in: R. Leegood, T. Sharkey, S. von Caemmerer (Eds.), Photosynthesis: Physiology and Metabolism, Kluwer Academic, Dordrecht, 2000, pp. 53–83.
[3] W.W. Cleland, T.J. Andrews, S. Gutteridge, F.C. Hartman, G.H. Lorimer, Mechanism of Rubisco: the carbamate as general base, Chem. Rev. 98 (1998) 549–562.
[4] F.R. Tabita, S. Satagopan, T.E. Hanson, N.E. Kreel, S.S. Scott, Distinct form I II, III, and IV Rubisco proteins from the three kingdoms of life provide clues about Rubisco evolution and structure/function relationships, J. Exp. Bot. 59 (2008) 1515–1524.
[5] M.R. Harpel, F.C. Hartman, Chemical rescue by exogenous amines of a site-directed mutant of ribulose 1,5-bisphosphate carboxylase/oxygenase that lacks a key lysyl residue, Biochemistry 33 (1994) 5553–5561.
[6] I. Andersson, A. Backlund, Structure and function of Rubisco, Plant Physiol. Biochem. 46 (2008) 275–291.
[7] H. Ashida, Y. Saito, T. Nakano, N. Tandeau de Marsac, A. Sekowska, A. Danchin, A. Yokota, RuBisCO-like proteins as the enolase enzyme in the methionine salvage pathway: functional and evolutionary relationships between RuBisCO-like proteins and photosynthetic RuBisCO, J. Exp. Bot. 59 (2008) 1543–1554.
[8] H. Ashida, A. Danchin, A. Yokota, Was photosynthetic RuBisCO recruited by acquisitive evolution from RuBisCO-like proteins involved in sulfur metabolism?, Res Microbiol. 156 (2005) 611–618.
[9] H. Ashida, Y. Saito, C. Kojima, K. Kobayashi, N. Ogasawara, A. Yokota, A functional link between RuBisCO-like protein of Bacillus and photosynthetic RuBisCO, Science 302 (2003) 286–290.
[10] T. Nakano, H. Ashida, E. Mizohata, H. Matsumura, A. Yokota, An evolutionally conserved Lys122 is essential for function in *Rhodospirillum rubrum* bona fide RuBisCO and *Bacillus subtilis* RuBisCO-like protein, Biochem. Biophys. Res. Commun. 392 (2010) 212–216.
[11] Y. Saito, H. Ashida, T. Sakiyama, N.T. de Marsac, A. Danchin, A. Sekowska, A. Yokota, Structural and functional similarities between a ribulose-1,5-bisphosphate carboxylase/oxygenase (RuBisCO)-like protein from *Bacillus subtilis* and photosynthetic RuBisCO, J. Biol. Chem. 284 (2009) 13256–13264.
[12] A. Carre-Mlouka, A. Mejean, P. Quillardet, H. Ashida, Y. Saito, A. Yokota, I. Callebaut, A. Sekowska, E. Dittmann, C. Bouchier, N.T. de Marsac, A new rubisco-like protein coexists with a photosynthetic rubisco in the planktonic cyanobacteria microcystis, J. Biol. Chem. 281 (2006) 24462–24471.
[13] H.J. Imker, A.A. Fedorov, E.V. Fedorov, S.C. Almo, J.A. Gerlt, Mechanistic diversity in the RuBisCO superfamily: the enolase in the methionine salvage pathway in *Geobacillus kaustophilus*, Biochemistry 46 (2007) 4077–4089.
[14] T.J. Erb, B.S. Evans, K. Cho, B.P. Warlick, J. Sriram, B.M. Wood, H.J. Imker, J.V. Sweedler, F.R. Tabita, J.A. Gerlt, A RubisCO-like protein links SAM metabolism with isoprenoid biosynthesis, Nat. Chem. Biol. 8 (2012) 926–932.
[15] H. Tamura, Y. Saito, H. Ashida, Y. Kai, T. Inoue, A. Yokota, H. Matsumura, Structure of the apo decarbamylated form of 2,3-diketo-5-methylthiopentyl-1-phosphate enolase from *Bacillus subtilis*, Acta Crystallogr., D Biol. Crystallogr. 65 (2009) 942–951.
[16] M.R. Harpel, F.W. Larimer, F.C. Hartman, Multiple catalytic roles of His 287 of *Rhodospirillum rubrum* ribulose 1,5-bisphosphate carboxylase/oxygenase, Protein Sci. 7 (1998) 730–738.
[17] M.M. Benning, J.M. Kuo, F.M. Raushel, H.M. Holden, Three-dimensional structure of the binuclear metal center of phosphotriesterase, Biochemistry 34 (1995) 7973–7978.
[18] N.C. Ha, S.T. Oh, J.Y. Sung, K.A. Cha, M.H. Lee, B.H. Oh, Supramolecular assembly and acid resistance of *Helicobacter pylori* urease, Nat. Struct. Biol. 8 (2001) 505–509.
[19] T. Lundqvist, G. Schneider, Crystal structure of the ternary complex of ribulose-1,5-bisphosphate carboxylase, Mg(II), and activator CO_2 at 2.3-A resolution, Biochemistry 30 (1991) 904–908.
[20] T.C. Taylor, I. Andersson, Structure of a product complex of spinach ribulose-1,5-bisphosphate carboxylase/oxygenase, Biochemistry 36 (1997) 4041–4046.
[21] G.H. Lorimer, M.R. Badger, T.J. Andrews, The activation of ribulose-1,5-bisphosphate carboxylase by carbon dioxide and magnesium ions. Equilibria, kinetics, a suggested mechanism, and physiological implications, Biochemistry 15 (1976) 529–536.
[22] W.A. Laing, J.T. Christeller, A model for the kinetics of activation and catalysis of ribulose 1,5-bisphosphate carboxylase, Biochem. J. 159 (1976) 563–570.
[23] J.T. Christeller, W.A. Laing, A kinetic study of ribulose bisphosphate carboxylase from the photosynthetic bacterium *Rhodospirillum rubrum*, Biochem. J. 173 (1978) 467–473.
[24] W.A. King, J.E. Gready, T.J. Andrews, Quantum chemical analysis of the enolization of ribulose bisphosphate: the first hurdle in the fixation of CO_2 by Rubisco, Biochemistry 37 (1998) 15414–15422.